A Novel and Efficient Implementation of Higher Order CPML for Truncating the Unmagnetized Plasma

Jianxiong Li[1, *], Zhi Li[1], and Xiaoming Zhao[2]

Abstract—A novel and efficient higher order convolutional perfectly matched layer (CPML) method is put forward and also applied to cut off the finite-difference time-domain (FDTD) computational domain full of the unmagnetized plasma. A Drude model can be used to represent the unmagnetized plasma, and the plasma can be solved by using the trapezoidal recursive convolution (TRC) method. In order to verify the validity of the presented method, a numerical example in three-dimensional computational domain is provided. The numerical example results show that the proposed formulations have better absorbing performance than the first-order CPML in terms of attenuating low-frequency and evanescent waves. Besides, by using the proposed method, computational time and memory can be reduced compared to the second order PML implemented by using the auxiliary differential equation (ADE) method.

1. INTRODUCTION

Since finite difference time domain (FDTD) method can directly settle the Maxwell's equations in time domain, FDTD method has been widely used in antennas, microwaves, electromagnetic imaging, and other fields. However, due to the restriction of computer memory, FDTD computation can only be performed in a limited region. To simulate the open problem, we need to use absorbing boundary conditions (ABCs) at the truncated boundary of the unbounded FDTD computational domain. Among many ABCs, perfectly matched layer (PML) [1] is a very effective and popular method for the termination of FDTD lattices. By converting Maxwell's equations to a complex stretching coordinate system, the stretched coordinate PML (SC-PML) with simple implementation has been put forward [2]. However, the SC-PML formulations are inefficient to absorb evanescent waves. To overcome the disadvantage, the convolutional PML (CPML) [3] was presented on the basis of the complex frequency shifted PML (CFS-PML) that has a rigorous causal mode [4, 5]. However, the absorption capacity of CFS-PML to low frequency propagation waves is poor. For the purpose of solving the above PML problems, the higher order PML with the advantages of SC-PML and CFS-PML was proposed in [6–9].

In this paper, we propose a novel method to implement the higher order CPML, named here as the 2nd-CPML, and use it to truncate the unmagnetized plasm. The 2nd-CPML is completely independent of the host medium. The constitutive relationship of the unmagnetized plasma can be settled by the trapezoidal recursive convolution (TRC) method [10]. To validate the proposed formulations, a numerical example in three-dimensional (3D) computational domain is provided. Through the results of the numerical example, we can clearly see that the 2nd-CPML can significantly enhance the absorption effect of the PML compared to the first order CPML, named here as the 1st-CPML [3]. Additionally, the 2nd-CPML can reduce the computational time and memory compared with the second order PML implemented by using the auxiliary differential equation (ADE) method, named here as the ADE 2nd-PML [8].

2. FORMULATIONS

In the PML regions for terminating unmagnetized plasma, in the frequency domain, the formulation for E_x component of Maxwell's equations can be written as follows

$$j\omega D_x = \frac{1}{S_y}\frac{\partial H_z}{\partial y} - \frac{1}{S_z}\frac{\partial H_y}{\partial z} \tag{1}$$

where $S_\eta(\eta = y, z)$ is the 2nd-CPML variables, defined as

$$S_\eta = \left(\kappa_{\eta 1} + \frac{\sigma_{\eta 1}}{\alpha_{\eta 1} + j\omega\varepsilon_0}\right)\left(\kappa_{\eta 2} + \frac{\sigma_{\eta 2}}{\alpha_{\eta 2} + j\omega\varepsilon_0}\right), \quad \eta = y, z \tag{2}$$

where $\sigma_{\eta\varphi}$ and $\alpha_{\eta\varphi}$, $\varphi = 1, 2$, are supposed to be positive real, and $\kappa_{\eta\varphi} \geq 1$ is real.

After some manipulations, one obtains

$$\frac{1}{S_\eta} = \kappa_{\eta 0} + \frac{w_{\eta 1}}{j\omega + v_{\eta 1}} + \frac{w_{\eta 2}}{j\omega + v_{\eta 2}} \tag{3}$$

where $\kappa_{\eta 0} = \frac{1}{\kappa_{\eta 1}\kappa_{\eta 2}}$, $w_{\eta 1} = \kappa_{\eta 0}[\frac{r_{\eta 1}r_{\eta 2}}{v_{\eta 2} - v_{\eta 1}} - r_{\eta 1}]$, $w_{\eta 2} = \kappa_{\eta 0}[-\frac{r_{\eta 1}r_{\eta 2}}{v_{\eta 2} - v_{\eta 1}} - r_{\eta 2}]$, $v_{\eta\varphi} = \frac{\alpha_{\eta\varphi}}{\varepsilon_0} + r_{\eta\varphi}$, and $r_{\eta\varphi} = \frac{\sigma_{\eta\varphi}}{\kappa_{\eta\varphi}\varepsilon_0}$.

The constitutive relation of the unmagnetized plasma with the Drude model is

$$D_x = \varepsilon_0\varepsilon_r(\omega) E_x \tag{4}$$

where

$$\varepsilon_r(\omega) = 1 + \frac{\omega_p^2}{-\omega^2 + j\omega v} \tag{5}$$

where ω_p and v represent the plasma frequency and the collision frequency, respectively.

Equation (4) can be solved by using the TRC method as

$$D_x^{n+1} - D_x^n = \varepsilon_0\left(1 + \frac{\chi^0}{2}\right)E_x^{n+1} - \varepsilon_0\left(1 - \frac{\chi^0}{2}\right)E_x^n - \varepsilon_0\psi_x^n \tag{6}$$

$$\psi_x^n = \frac{\Delta\chi^0}{2}\cdot\left(E_x^n + E_x^{n-1}\right) + \exp\left(-v\Delta t\right)\psi_x^{n-1} \tag{7}$$

where $\chi^0 = \frac{\omega_p^2\Delta t}{v} - \frac{\omega_p^2}{v^2}\cdot[1 - \exp(-v\Delta t)]$, $\Delta\chi^0 = -\frac{\omega_p^2}{v^2}\cdot[1 - \exp(-v\Delta t)]^2$, and Δt is time step.

After transforming Equation (1) into the time domain, there is a convolution on the right side due to the frequency dependence of S_η, namely

$$\frac{\partial D_x}{\partial t} = \overline{S_y}(t) * \frac{\partial H_z}{\partial y} - \overline{S_z}(t) * \frac{\partial H_y}{\partial z} \tag{8}$$

where $\overline{S_\eta}(t)$ is the inverse Laplace transform of S_η^{-1} given as

$$\overline{S_\eta}(t) = \kappa_{\eta 0}\delta(t) + \zeta_{\eta 1}(t) + \zeta_{\eta 2}(t) \tag{9}$$

In the above the equation, $\delta(t)$ is the unit pulse function, $\zeta_{\eta\varphi}(t) = w_{\eta\varphi}\exp(-v_{\eta\varphi}t)u(t)$, where $u(t)$ is unit step function. Like the method in [3], by substituting Eq. (9) into Eq. (8) and introducing the auxiliary variables, one obtains

$$\frac{\partial D_x}{\partial t} = \kappa_{y0}\cdot\frac{\partial H_z}{\partial y} + F_{xy1} + F_{xy2} - \kappa_{z0}\cdot\frac{\partial H_y}{\partial z} - F_{xz1} - F_{xz2} \tag{10}$$

Through calculating the auxiliary variables recursively [3] and discretizing by the FDTD method, one obtains

$$F_{xy\phi}^{n+\frac{1}{2}}\left(i+\frac{1}{2}, j, k\right) = g_{y\phi}(j)F_{xy\phi}^{n-\frac{1}{2}}\left(i+\frac{1}{2}, j, k\right) + h_{y\phi}(j)\left(H_z^{n+\frac{1}{2}}\left(i+\frac{1}{2}, j+\frac{1}{2}, k\right) - H_z^{n+\frac{1}{2}}\left(i+\frac{1}{2}, j-\frac{1}{2}, k\right)\right) \tag{11}$$

$$F_{xz\phi}^{n+\frac{1}{2}}\left(i+\frac{1}{2},j,k\right) = g_{z\phi}(k)\, F_{xz\phi}^{n-\frac{1}{2}}\left(i+\frac{1}{2},j,k\right) + h_{z\phi}(k)\left(H_y^{n+\frac{1}{2}}\left(i+\frac{1}{2},j,k+\frac{1}{2}\right) - H_y^{n+\frac{1}{2}}\left(i+\frac{1}{2},j,k-\frac{1}{2}\right)\right)$$
(12)

where $g_{\eta\varphi} = \exp(-v_{\eta\varphi} \cdot \Delta t)$, $h_{\eta\varphi} = \frac{w_{\eta\varphi}(1-g_{\eta\varphi})}{v_{\eta\varphi}\Delta\eta}$, and $\Delta\eta$ is space step.

After Eq. (10) is discretized, inserting Eq. (6) into it, and after some simple manipulations, one obtains

$$E_x^{n+1}\left(i+\frac{1}{2},j,k\right)$$

$$= c_1 E_x^n\left(i+\frac{1}{2},j,k\right) + c_2\psi_x^n\left(i+\frac{1}{2},j,k\right)$$

$$+p_y(j)\left(H_z^{n+\frac{1}{2}}\left(i+\frac{1}{2},j+\frac{1}{2},k\right) - H_z^{n+\frac{1}{2}}\left(i+\frac{1}{2},j-\frac{1}{2},k\right)\right)$$

$$-p_z(k)\left(H_y^{n+\frac{1}{2}}\left(i+\frac{1}{2},j,k+\frac{1}{2}\right) - H_y^{n+\frac{1}{2}}\left(i+\frac{1}{2},j,k-\frac{1}{2}\right)\right)$$

$$+c_3\left(F_{xy1}^{n+\frac{1}{2}}\left(i+\frac{1}{2},j,k\right) + F_{xy2}^{n+\frac{1}{2}}\left(i+\frac{1}{2},j,k\right) - F_{xz1}^{n+\frac{1}{2}}\left(i+\frac{1}{2},j,k\right) - F_{xz2}^{n+\frac{1}{2}}\left(i+\frac{1}{2},j,k\right)\right) \quad (13)$$

where $c_1 = c_2(1 - \frac{\chi^0}{2})$, $c_2 = (1 + \frac{\chi^0}{2})^{-1}$, $c_3 = \frac{c_2\Delta t}{\varepsilon_0}$, and $p_\eta = \frac{c_3\kappa_{\eta 0}}{\Delta\eta}$.

By using a similar method, for example, the magnetic field component H_z can also be given as

$$H_z^{n+\frac{1}{2}}\left(i+\frac{1}{2},j+\frac{1}{2},k\right)$$

$$= H_z^{n-\frac{1}{2}}\left(i+\frac{1}{2},j+\frac{1}{2},k\right) + q_y\left(j+\frac{1}{2}\right)\left(E_x^n\left(i+\frac{1}{2},j+1,k\right) - E_x^n\left(i+\frac{1}{2},j,k\right)\right)$$

$$-q_x\left(i+\frac{1}{2}\right)\left(E_y^n\left(i+1,j+\frac{1}{2},k\right) - E_y^n\left(i,j+\frac{1}{2},k\right)\right)$$

$$+c_h\left(G_{zy1}^n\left(i+\frac{1}{2},j+\frac{1}{2},k\right) + G_{zy2}^n\left(i+\frac{1}{2},j+\frac{1}{2},k\right)\right.$$

$$\left.-G_{zx1}^n\left(i+\frac{1}{2},j+\frac{1}{2},k\right) - G_{zx2}^n\left(i+\frac{1}{2},j+\frac{1}{2},k\right)\right)$$
(14)

where $q_\eta = \frac{\Delta t\kappa_{\eta 0}}{\mu_0\Delta\eta}$ and $c_h = \frac{\Delta t}{\mu_0}$.

A similar method can be used to calculate other components. Like the 1st-CPML [3], and the 2nd-CPML is also fully independent of the host medium.

To compare the proposed 2nd-CPML with the ADE 2nd-PML [8] in terms of computational time, we assume the PMLs truncate a 3D vacuum FDTD computational domain. The 2nd-CPML requires 11 multiplications and 16 additions to obtain E_x, but the ADE 2nd-PML requires 14 multiplications and 12 additions. Since the computational time of the multiplication is longer than that of the addition, the 2nd-CPML consumes less computational time than the ADE 2nd-PML.

3. NUMERICAL RESULTS

To validate the proposed 2nd-CPML method for terminating unmagnetized plasma, a numerical example in 3D domain is provided. The computational domain is a $30\times30\times30$ uniform mesh domain that is fully filled with the unmagnetized plasma with the parameters of $\omega_p = 2\pi \times 28.7\,\mathrm{Grad/s}$ and $v = 20\,\mathrm{GHz}$, and it is truncated by the 8-cell-PML. The FDTD lattice is $\Delta x = \Delta y = \Delta z = \Delta = 0.215\,\mathrm{mm}$. The time step can be easily calculated by $\Delta t = \Delta/\sqrt{3}c$, where c is the speed of light, so $\Delta t = 0.4\,\mathrm{ps}$. The observation point is set in the corner of the computational domain with the distance of a cell from three

faces of the PML. The modulated Gaussian pulse is used as the excitation source with the parameters of the maximum frequency of 70 GHz and the center frequency of 30 GHz, and it is placed at the middle of the FDTD computational domain. The parameters of the 2nd-CPML are chosen as $m_1 = 4$, $\alpha_1 = 5$, $\sigma_{1\max} = 0.1\sigma_{1opt}$, $k_{1\max} = 1$, $m_2 = 2$, $\alpha_2 = 1.1$, $\sigma_{2\max} = 1.3\sigma_{2opt}$, $k_{2\max} = 2$, where $\sigma_{\varphi opt}$ is given as $\sigma_{\varphi opt} = (m_\varphi + 1)/150\pi\Delta$. For comparison, the 1st-CPML with the parameters of $m = 3$, $\alpha = 0.4$, $\sigma_{\max} = 2.0\sigma_{opt}$, $k_{\max} = 13$ and the ADE 2nd-PML with $m_1 = 3$, $\alpha_1 = 4.6$, $\sigma_{1\max} = 0.3\sigma_{1opt}$, $k_{1\max} = 7$, $m_2 = 2$, $\alpha_2 = 1$, $\sigma_{2\max} = 1.1\sigma_{2opt}$, $k_{2\max} = 2$ are also implemented. These parameters have been optimized by looping through a large number of different parameters to obtain the best absorption performance.

To evaluate the performance of the PML, we use the relative reflection error in the time domain and the reflection coefficient in the frequency domain, which are defined as

$$R_{\mathrm{dB}}(t) = 20\log_{10}\left|\frac{E_x^T(t) - E_x^R(t)}{\max\{E_x^R(t)\}}\right| \tag{15}$$

$$R_{\mathrm{dB}}(f) = 20\log_{10}\left|\frac{FFT\{E_x^T(t) - E_x^R(t)\}}{FFT\{E_x^R(t)\}}\right| \tag{16}$$

where $FFT\{\}$ indicates the Fourier transform, and $E_x^T(t)$ and $E_x^R(t)$ represent the test solutions and reference solutions, respectively. To obtain the reference solution, the FDTD computational domain is expanded to $80 \times 80 \times 80$ uniform mesh domain and terminated by the 32-cell-PML.

Figure 1 and Figure 2 show the relative reflection errors and reflection coefficients of the 1st-CPML, 2nd-CPML, and the ADE 2nd-PML, respectively. Meanwhile, we use the biggest relative reflection error (BRRE) and biggest reflection coefficient (BRC) to evaluate the absorbing performance of the PML in Table 1. As can be seen from Table 1, Figure 1, and Figure 2, compared with the 1st-CPML, the
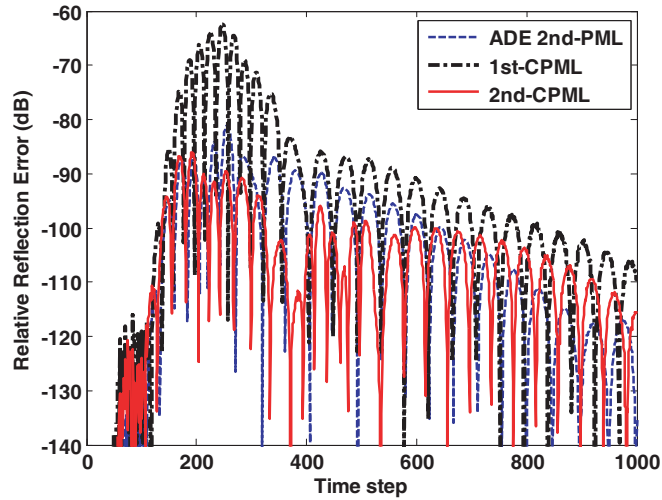
Figure 1. Relative reflection errors.

Table 1. Computation time, memory, BRRE and BRC of 1st-CPML, 2nd-CPML and ADE 2nd-CPML to truncate unmagnetized plasma.

	Time (s)	Memory (MB)	BRRE (dB)	BRC (dB)
1st-CPML (PML = 8)	70.0	80.5	-64.46	-52.23
2nd-CPML (PML = 8)	101.56	83.6	-87.74	-75.93
2nd-CPML (PML = 4)	59.2	67.4	-68.51	-56.47
ADE 2nd-PML (PML = 8)	121.20	105.4	-80.93	-58.66
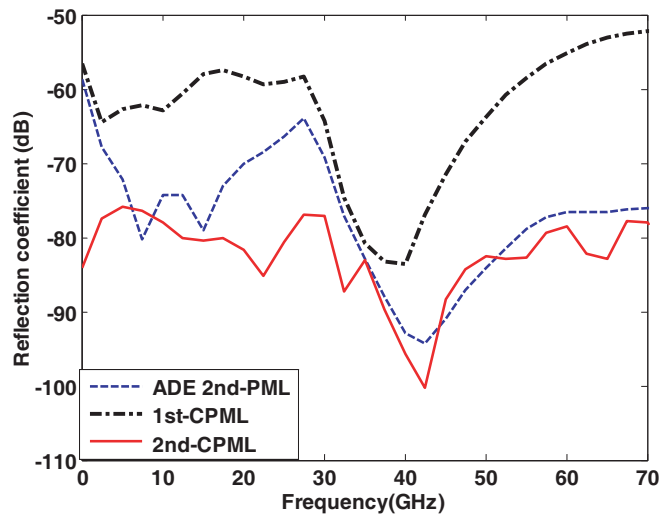
Figure 2. Reflection coefficients.

2nd-CPML significantly improves the absorption performance including the low-frequency propagation wave although it costs more computational time and a little more memory. However, we can also see that when PML = 4, the 2nd-CPML can cost less time and memory to achieve a little better absorption performance than the 1st-CPML. Compared to the ADE 2nd-PML, the 2nd-CPML has a little better absorption performance, especially at low frequency, and consumes less computational time and memory. In other words, the implementation of the 2nd-CPML is efficient.

4. CONCLUSION

The efficient 2nd-CPML is proposed and also applied to truncate unmagnetized plasma solved by the TRC method. In order to validate the proposed method, a numerical example in 3D computational domain is presented. It can be shown that the proposed algorithm has a very good absorbing effect in truncating the unmagnetized plasma through the numerical results. Moreover, the proposed algorithm requires less computational resource than the ADE 2nd-PML method [8].

ACKNOWLEDGMENT

REFERENCES

1. Berenger, J. P., "A perfectly matched layer for the absorption of electromagnetic waves," *J. Comput. Phys.*, Vol. 114, No. 2, 185–200, 1994.
2. Chew, W. C. and W. H. Weedon, "A 3D perfectly matched medium from modified Maxwell's equations with stretched coordinates," *Microw. Opt. Technol. Lett.*, Vol. 7, No. 13, 599–604, 1994.
3. Roden, J. A. and S. D. Gedney, "Convolution PML (CPML): An efficient FDTD implementation of the CFS-PML for arbitrary media," *Microw. Opt. Technol. Lett.*, Vol. 27, No. 5, 334–339, 2000.
4. Kuzuoglu, M. and R. Mittra, "Frequency dependence of the constitutive parameters of causal perfectly matched anisotropic absorbers," *IEEE Microwave and Guided Wave Letters*, Vol. 6, No. 12, 447–449, 1996.
5. Berenger, J. P., "Numerical reflection from FDTD-PMLs: A comparison of the split PML with the unsplit and CFSPMLs," *IEEE Trans. Antennas Propag.*, Vol. 50, No. 3, 258–265, 2002.

6. Correia, D. and J. M. Jin, "Performance of regular PML, CFS-PML, and second-order PML for waveguide problems," *Microw. Opt. Technol. Lett.*, Vol. 48, No. 10, 2121–2126, 2006.

7. Gedney, S. D. and B. Zhao, "An auxiliary differential equation formulation for the complex-frequency shifted PML," *IEEE Trans. Antenna Propag.*, Vol. 58, No. 3, 838–847, 2010.

8. Feng, N. X. and J. X. Li, "Novel and efficient FDTD implementation of higher-order perfectly matched layer based on ADE method," *J. Comput. Phys.*, Vol. 232, No. 1, 318–326, 2013.

9. Li, J. X., P. Y. Wu, and H. L. Jiang, "Implementation of higher order CNAD CFS-PML for truncating unmagnetized plasma," *IET Microw. Antennas Propag.*, Vol. 13, No. 6, 756–760, 2018.

10. Liu, S., S. Q. Liu, and S. B. Liu, 'Finite-difference time-domain algorithm for plasma based on trapezoidal recursive convolution technique," *J. Infrared. Millim. Te.*, Vol. 31, No. 5, 620–628, 2010.